Inorganica Chimica Acta 363 (2010) 2696–2701

Contents lists available at ScienceDirect

Inorganica Chimica Acta

journal homepage: www.elsevier.com/locate/ica

Nanorods and nanofilms of ZnO generated at the liquid–liquid interface

S. Manjunatha, L.S. Panchakarla, Kanishka Biswas, C.N.R. Rao *

International Centre for Materials Science, Chemistry and Physics of Materials Unit, and CSIR Centre of Excellence in Chemistry, Jawaharlal Nehru Centre for Advanced Scientific Research, Jakkur P.O. Bangalore 560064, India

ARTICLE INFO

Article history:
Received 18 January 2010
Accepted 22 February 2010

Dedicated to Prof. Animesh Chakravorty

Keywords:
Zno
Nanostructures
Liquid–Liquid interface
Magnetic properties

ABSTRACT

Reaction between zinc cupferron and alkali at the organic–aqueous interface has been investigated in detail. In the presence of an organic amine, this reaction yields ZnO nanorods, the morphology depending on the concentration of reactants. In the absence of the amine, ultrathin films of ZnO are produced. Amazingly, both the nanorods and thin films are single crystalline in nature, even though the synthesis is carried out at room-temperature. Single-crystalline, substrate-free ultrathin films of ZnO, is indeed an extraordinary feature of synthesis at the liquid–liquid interface. Photoluminescence spectra show defect-related bands besides that due to band edge emission. The nanostructures exhibit ferromagnetism due to surface defects.

1. Introduction

It has been shown recently that the liquid–liquid (organic–aqueous) interface can be exploited to generate nanocrystalline films of a variety of inorganic materials such as metals, metal alloys, and metal chalcogenides [1–4]. Nanocrystalline films synthesised at the interface are 40–80 nm thick and generally consist of small nanocrystalline particles. In some instances, the films are single-crystalline, as exemplified by CuS [2]. Nonlinear visco–elastic properties, interfacial rheology of such ultrathin nanocrystalline films generated by this method have been studied [5,6]. The liquid–liquid interface method involves taking an organo-metallic compound in the organic phase and the relevant reactant in the aqueous phase. The reaction occurs at the interface giving rise to ultrathin films or different nanostructures depending on the concentration of the reactants. Adding a small concentration of surfactant to the organic or aqueous phase affects the morphology of the nanostructures formed at the interface [7]. We considered it important to investigate ZnO nanostructures formed at the liquid–liquid interface, in view of their potential applications in optical, electronic and optoelectronic devices [8–11]. ZnO is an important semi-conducting material with a band gap of 3.37 eV at room temperature, and a relatively high exciton binding energy of 60 meV, exhibiting near-UV emission, transparent conductivity, and piezoelectricity and such interesting properties. The high electron mobility and visible transparency of ZnO thin films helps to use in thin film transistors, UV detectors, UV and blue light emitting diodes (LEDs) and laser diodes [12]. ZnO nanorods can be used as photo detectors, LEDs, field effect transistors (FETs) and sensors [13–18]. Several methods have been employed to synthesise the ZnO nanostructures which include both physical and chemical methods [19,20]. For instance, ZnO nanorods can be prepared by CVD [21,22], solvothermal methods [23,24] and reaction of zinc metal with water [25]. ZnO nanofilms can be prepared by standard methods employed for thin films such as chemical vapour deposition, pulsed laser deposition and electrodeposition [26–28]. None of these methods produces thin single-crystalline films. We felt that the liquid–liquid interface may provide nanofilms as well as other nanostructures of ZnO with novel morphologies and properties. In this article we present the synthesis and properties of ultrathin films and other nanostructures of ZnO generated at the liquid–liquid interface. Interestingly both the films and nanorods are formed to be single-crystalline.

2. Experimental

2.1. Synthesis of ZnO nanorods at the liquid–liquid interface

The procedure to prepare ZnO nanorods at the liquid–liquid interface involved taking the zinc(II) cupferron ($Zn(Cup)_2$) as the zinc source in the toluene phase, and NaOH as the reactant in the water phase. $Zn(cup)_2$ was prepared by the reaction of cupferron with zinc acetate in water at 273 K, then filtered and dried in a vacuum tube. $Zn(cup)_2$ along with appropriate amount of an organic amine in toluene was added to the NaOH aqueous phase with

DOI of original article: 10.1016/j.ica.2010.02.025
* Corresponding author. Fax: +91 80 22082760.
E-mail address: cnrrao@jncasr.ac.in (C.N.R. Rao).

0020-1693/$ - see front matter © 2010 Elsevier B.V. All rights reserved.
doi:10.1016/j.ica.2010.09.008

suitable pH. The reactions at the interface were all carried out at 303 K.

To examine the effect of OH^- concentration relative to Zn^{2+} concentration, we kept the trioctylamine concentration constant at 4.58 mM and varied the concentration ratio between Zn^{2+} and OH^-. In a typical experiment, we have taken 25 mL of 0.04 M NaOH solution in three separate 100 mL beakers (pH ~ 12). To these, we added 2, 10 and 20 mg of $Zn(cup)_2$ in 25 mL of toluene containing 4.58 mM trioctylamine, so that the actual concentrations of $Zn(Cup)_2$ were 0.24, 1.18, 2.36 mM respectively. The interface attains a white colour after a few hours indicating the formation of ZnO nanostructures. The thickness of the layer at the interface increases with time. After 10 h, the organic phase was removed and the film containing ZnO nanostructures carefully lifted on to a silicon substrate for characterisation.

In order to study the effect of chain length of the amine on the nanorods, we kept the $Zn(Cup)_2$ concentration in the organic phase at 0.24 mM, and 0.04 M NaOH in the aqueous phase constant. Different amines were added to the organic phase to attain an actual concentration of 2.29 mM. The amines used were *n*-butylamine, *n*-octylamine, *n*-dodecyl amine and *n*-hexadecyl amine. We also studied the effect of amine concentration on nanorods formation. For this purpose, we took 2.36 mM $Zn(Cup)_2$ in the organic phase and 0.04 M NaOH in the aqueous phase in three separate beakers. The concentration of the trioctylamine in the organic phase was varied as 2.29, 4.58 and 18.32 mM.

2.2. Synthesis of ZnO thin films at the liquid–liquid interface

For preparing thin films of ZnO, we took 25 mL of 0.04 M of NaOH in a 100 mL beaker, to which 25 mL of 0.12 mM $Zn(Cup)_2$ in toluene was added slowly at 303 K. The interface attains a white colour after a few hours, and a distinct film is formed after 10 h.

2.3. Characterisation

All the samples were examined by X-ray diffraction using Cu Kα radiation (λ = 1.54056 Å) using a Rigaku-99 instrument. The morphology of the samples ware studied by using a field emission scanning electron microscope (FESEM – FEI NOVA NANOSEM 600) and a transmission electron microscope (TEM – JEOL JEM 3010) images. UV–Vis absorption spectra were recorded using a Perkin–Elmer Lamda 900 UV/Vis/NIR spectrometer. Photoluminescence (PL) spectra were recorded with a Perkin–Elmer model LS55 luminescence spectrometer. Atomic force microscope (AFM) measurements were performed using NanoMan. Magnetic measurements were carried out with vibrating sample magnetometer in Physical Properties Measurement System (PPMS, Quantum Design, USA).

3. Results and discussion

We first studied the effects of concentrations of the zinc precursor, $Zn(cup)_2$, NaOH as well as the organic amine on the ZnO nanostructures formed at the liquid–liquid interface. XRD patterns of the ZnO nanostructures obtained at the liquid-liquid interface could all be indexed on the hexagonal wurtzite structure (space group: $P6_3mc$; a = 0.3249 nm, c = 0.5206 nm, JCPDS card No. 36-1451). In the presence of an amine such as trioctylamine (TOA), the reaction between the $Zn(cup)_2$ and NaOH primarily yields nanorods. Fig. 1 shows FESEM images of the nanorods obtained with varying concentrations of $Zn(cup)_2$, keeping NaOH (0.04 M)

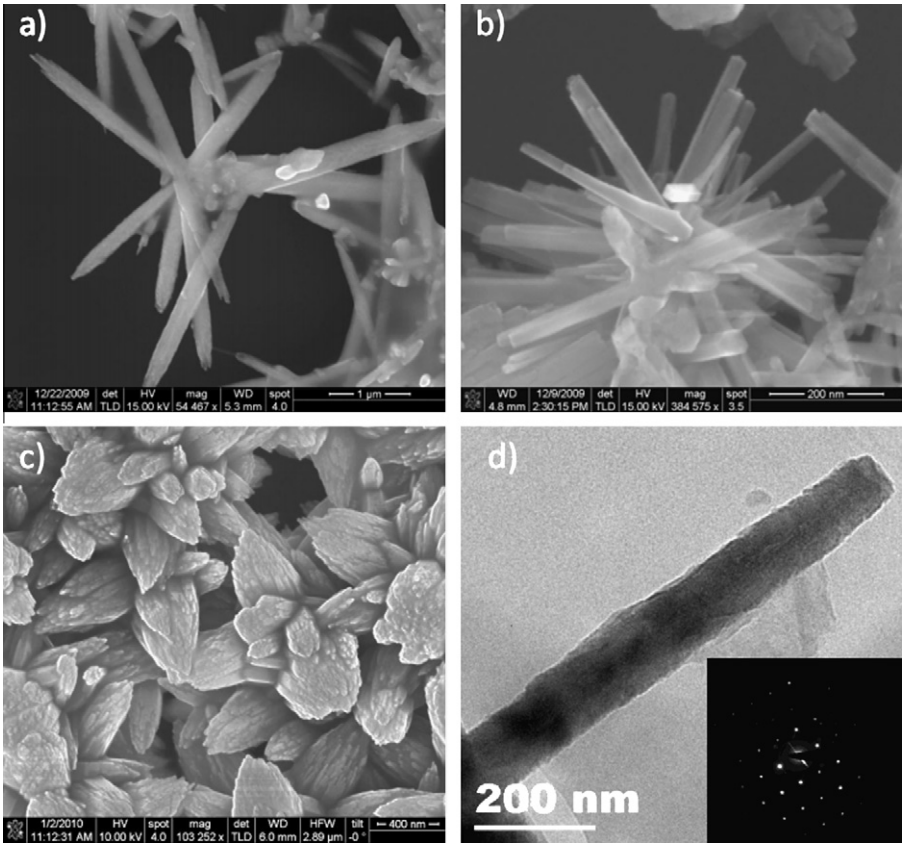

Fig. 1. FESEM images of ZnO nanorods, with variation of the concentration of zinc $(cup)_2$: (a) 0.24 mM, (b) 1.17 mM, and (c) 2.36 mM with a fixed concentration of NaOH (0.04 M), trioctyl amine (4.58 mM). (d) TEM image of a ZnO nanorod along with the SAED pattern.

and amine (4.58 mM) concentrations constant. When the $Zn(cup)_2$ concentration was 0.24 mM, well-defined nanorods of ZnO were formed at the interface as seen in Fig. 1a, the average diameter of the nanorods being around 250 nm with lengths up to 2–3 μm. In Fig. 1b and c, we show FESEM images of ZnO nanorods obtained with the $Zn(cup)_2$ concentrations of 1.17 and 2.36 mM respectively. The corresponding diameters of the nanorods obtained are 30 and 20 nm with lengths of around 300 and 450 nm respectively. At lower concentrations of $Zn(cup)_2$ relative to NaOH, the nanorods are less agglomerated but at the higher concentrations bundles of nanorods with agglomerated structures are obtained. Furthermore, as the relative concentration of $Zn(cup)_2$ is increased, the diameters of the synthesised nanorods decreases. All the nanorods obtained at the liquid–liquid interface, are generally single-crystalline. A typical TEM image of a ZnO nanorod synthesised using 0.24 mM of $Zn(Cup)_2$ is shown in Fig. 1d. The selected area electron diffraction (SAED) pattern shows the single-crystalline nature of nanorods (see inset of Fig. 1d). It is remarkable that the nanorods formed at room-temperature at the liquid–liquid interface are single-crystalline without involvement of vapour or liquid.

The bundle of nanorods prepared using a high concentration of $Zn(cup)_2$ of 2.36 mM, shows an absorption band at 367 nm (Fig. 2a) due to the smaller size of nanorods compared to those prepared by using less concentration of $Zn(cup)_2$ of 0.24 mM, which show a band at 370 nm (see inset of Fig. 2a). Room-temperature PL spectra of bundles of ZnO nanorod bundles (Fig. 2b) shows a weak UV emission band at 382 nm along with emission in the visible region. The UV emission is due to the radiative recombination between the electrons in the conduction band and the holes in the valence band. The bands around 404 and 425 nm are due to Zn vacancies (V_{Zn}) and Zn interstitials (Zn_i) respectively [29–31]. We also see a feature around 450 nm the origin of which is not clear [31,32]. The weak band around 550 nm is due to the localised levels in the band gap. The most probable origin for green emission lies in the oxygen vacancies [32]. Nanorods prepared using a lower concentration of $Zn(cup)_2$ (0.24 mM) show little difference in the PL spectrum. They show negligible band edge as well as green emissions, but show a strong emission at 404 and 425 nm in the violet region as seen in the inset of Fig. 2b. It is to be noted that V_{zn} and Zn_i quench the band edge emission.

The effect of amine chain length on the ZnO nanostructures formed at the liquid–liquid interface was studied by keeping $Zn(cup)_2$ and NaOH concentrations constant at 0.24 mM and 0.04 M respectively and the amine concentration at 4.58 mM. The amines studied were *n*-butylamine, *n*-octylamine, *n*-dodecylamine and *n*-hexadecylamine. In Fig. 3a and b, we show the FESEM images of nanorods at the interface using butylamine and hexadecylamine respectively. The morphology is not sensitive to the chain length of the amine. The corresponding PL spectra are shown in Fig. 3c and d respectively. As the chain length of the amine increases, one notices a decrease in the oxygen defect band intensity (550 nm).

We have studied the effect of concentration of the amine on the ZnO nanostructures by keeping the concentration of $Zn(cup)_2$ (1.17 mM) and NaOH (0.04 M) constant. In Fig. 4a–c, we have shown FESEM images of the nanorods obtained at the interface using TOA concentrations of 2.29, 4.58 and 18.32 mM respectively. The average diameters of the nanorods obtained with the amine concentrations are 200, 30 and 20 nm and corresponding lengths are 500, 300 and 800 nm respectively. It is interesting that, as the amine concentration is increased, the aspect ratio of the nanorods increases. PL spectra of these samples were similar (as in Fig. 2b). Fig. 4d shows a TEM image of the bundles of ZnO nanorods. The nanorods are single-crystalline as confirmed by the SAED pattern shown as an inset in Fig. 4d.

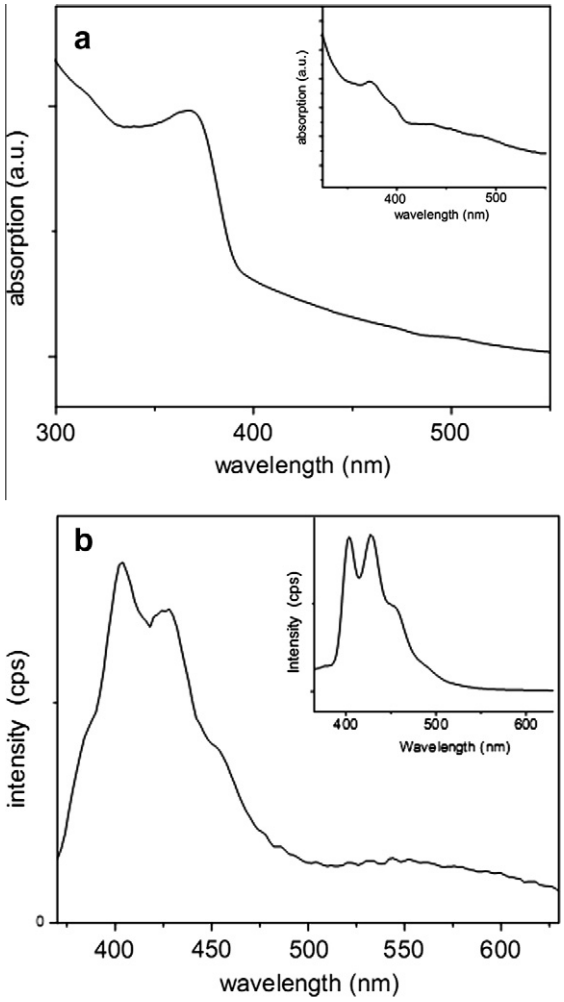

Fig. 2. (a) UV–Vis absorption spectrum of ZnO nanorods obtained with 2.36 mM of $Zn(cup)_2$ and 0.04 M NaOH and inset shows ZnO nanorods obtained at 0.24 mM of $Zn(cup)_2$. (b) PL spectrum of ZnO nanorods obtained with 2.36 mM of $Zn(cup)_2$ and inset shows ZnO nanorods obtained at 0.24 mM of $Zn(cup)_2$.

In the absence of an amine, we obtain ultrathin films of ZnO at the liquid–liquid interface when the concentration of $Zn(cup)_2$ was sufficiently low. This method enables us to obtain substrate-free films of ZnO. The as-synthesised ZnO films at the interface are readily transferred on to any solid substrate. A TEM image of a film obtained with a $Zn(cup)_2$ concentration 0.12 mM and a NaOH concentration of 0.04 M is shown in Fig. 5a. The SAED pattern reveals that the films were single-crystalline which is noteworthy. A situation similar to this has been reported in the case of CuS [1,6]. A contact mode AFM image of the ZnO thin film taken on a Si substrate is shown in Fig. 5b. The image reveals a film over an area of nearly 1 μm × 1 μm and its surface topology. The height profile in Fig. 5d shows the ZnO film have to have a thickness of 20 nm. This is indeed a unique feature of the film generated at the liquid–liquid interface. The PL spectrum depicted in Fig. 5c, shows a weak band edge emission at 382 nm and defect bands at 404 and 424 nm along with a weak band at 450 nm. The inset in Fig. 5c shows the UV–Vis absorption peak at around 370 nm. When the concentration of $Zn(cup)_2$ was high, we obtain ZnO nanorods even in the absence of amine. The FESEM image of such nanorods is shown in Fig. 6a. The PL spectrum (Fig. 6b) of these nanorods is similar to that of the nanorods obtained by using an amine shown earlier in Fig. 2b. The UV–Vis absorption spectrum shows the characteristic band of ZnO around 370 nm (see inset of Fig. 6b).

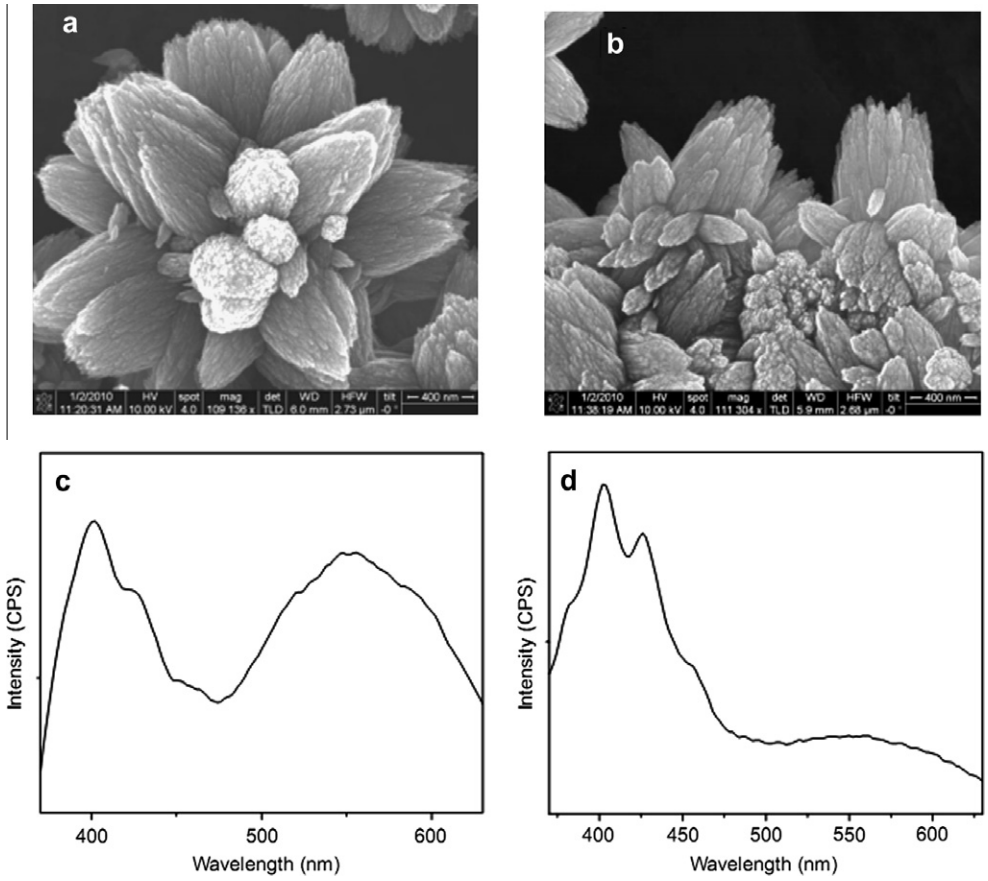

Fig. 3. FESEM images of ZnO nanoflowers obtained with 2.36 mM of $Zn(cup)_2$, 0.04 M of NaOH with variation of amine chain length using (a) butylamine and (b) hexadecyl amine, of concentrations 2.29 mM. The corresponding PL spectra of ZnO nanoflowers prepared using (c) butyl amine and (d) hexadecylamine.

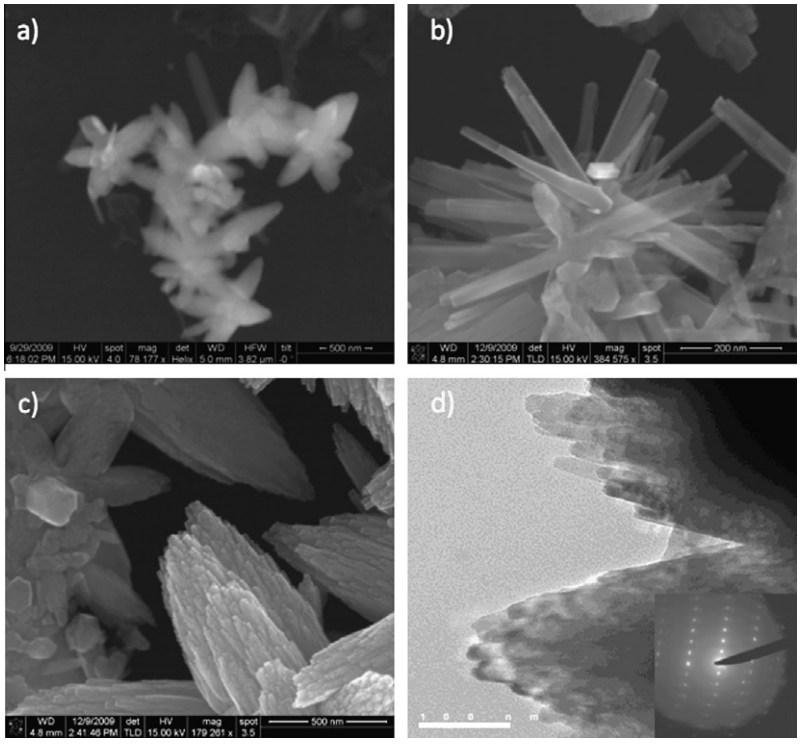

Fig. 4. FESEM images of ZnO nanorods obtained with 1.17 mM of $Zn(cup)_2$ 0.04 M of NaOH, with the variation of trioctyl amine concentration (a) 2.29 mM, (b) 4.58 mM, (c) 18.32 mM and (d) TEM image of bundles of ZnO nanorods obtained at trioctyl amine concentration 18.32 mM, along with SAED pattern.

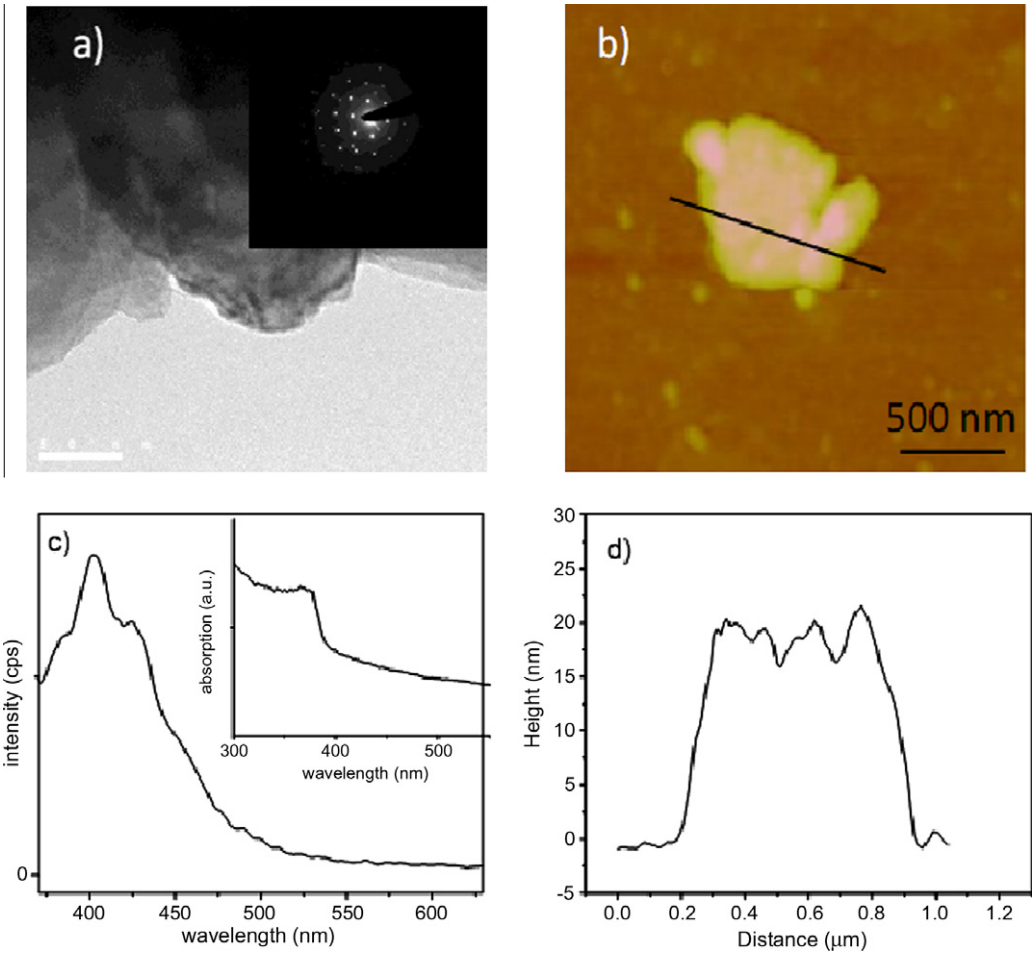

Fig. 5. ZnO single-crystalline ultrathin films obtained with 0.12 mM of $Zn(cup)_2$ and 0.04 M NaOH. (a) TEM image along with SAED pattern, (b) contact mode AFM image, (c) PL spectrum with inset UV–Vis absorption spectrum and (d) height profile of thin film obtained by AFM.

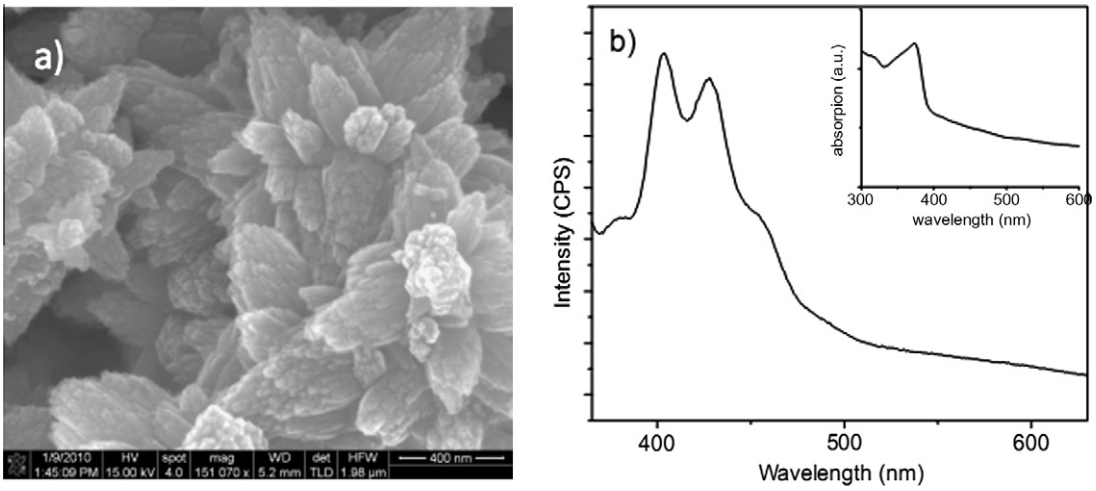

Fig. 6. (a) FESEM image of ZnO bundles of nanorods obtained with 2.36 mM of $Zn(cup)_2$ 0.04 M NaOH and (b) corresponding PL spectrum along with UV–Vis absorption spectrum as an inset.

The nanostructures of ZnO obtained at the liquid–liquid interface show a ferromagnetic hysteresis loop characteristic of metal oxide nanoparticles [33–35]. The magnetisation data of the film prepared at the liquid-liquid interface is shown in Fig. 7, as an example. The value of saturation magnetisation is 0.18 emu/g. The magnetism is clearly due to the defects on the surface of the nanostructures. Anion or cation vacancies and Zn interstitials all seem to lead to surface ferromagnetism.

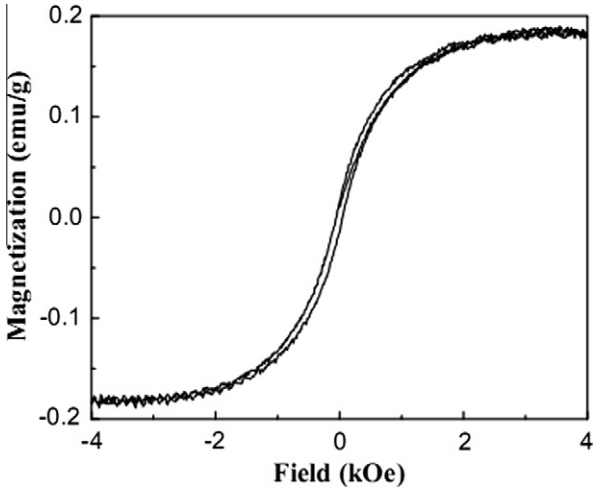

Fig. 7. Ferromagnetic hysteresis loop of ZnO thin film, obtained at the liquid–liquid interface using 0.12 mM of $Zn(cup)_2$ and 0.04 M of NaOH.

4. Conclusions

It is gratifying that one can prepare nanostructures of important oxides such as ZnO at the liquid–liquid interface. The nanostructures of ZnO produced at the interface include both one-dimensional nanorods and two-dimensional thin films, while both the nanorods and films are single-crystalline, a feature that is noteworthy. The ZnO films are extremely thin, obtaining such films by other means is difficult. All the nanostructures exhibit defect-related emission bands and magnetism. ZnO nanostructures produced at the interface may find applications in different areas.

Acknowledgement

One of the authors (L.S. Panchakarla) thanks CSIR for senior research fellowship.

References

[1] C.N.R. Rao, G.U. Kulkarni, P. Thomas, V.V. Agrawal, P. Saravannan, J. Phys. Chem. B 107 (2003) 7391.
[2] U.K. Gautam, M. Ghosh, C.N.R. Rao, Langmuir 20 (2004) 10775.
[3] C.N.R. Rao, G.U. Kulkarni, V.V. Agrawal, U.K. Gautham, M. Ghosh, U. Tumkurkar, J. Colloid Interface Sci. 289 (2005) 305.
[4] C.N.R. Rao, K.P. Kalyanikutty, Acc. Chem. Res. 41 (2008) 489.
[5] R. Krishnaswamy, S. Majumdar, R. Ganapathy, V.V. Agrawal, A.K. Sood, C.N.R. Rao, Langmuir 23 (2007) 3084.
[6] R. Krishnaswamy, K.P. Kalyanikutty, K. Biswas, A.K. Sood, C.N.R. Rao, Langmuir 25 (2009) 10954.
[7] V.V. Agrawal, G.U. Kulkarni, C.N.R. Rao, J. Colloid Interface Sci. 318 (2008) 501.
[8] R.F. Service, Science 276 (1997) 895.
[9] S.C. Minne, S.R. Manalis, C.F. Quate, Appl. Phys. Lett. 67 (1995) 3918.
[10] M.H. Huang, S. Mao, H. Feick, H. Yan, Y. Wu, H. Kind, E. Weber, R. Russo, P. Yang, Science 292 (2001) 1897.
[11] Z.L. Wang, Mater. Today 7 (2004) 26.
[12] D.M. Bagnall, Y.F. Chen, Z. Zhu, T. Yao, M.Y. Shen, T. Goto, Appl. Phys. Lett. 73 (1998) 1038.
[13] D. Appell, Nature 419 (2002) 553.
[14] K. Keem, H. Kim, G.T. Kim, J.S. Lee, B. Min, K. Cho, M.Y. Sung, S. Kim, Appl. Phys. Lett. 84 (2004) 4376.
[15] O. Harnack, C. Pacholski, H. Weller, A. Yasuda, J.M. Wessels, Nano Lett. 3 (2003) 1097.
[16] H. Kind, H.Q. Yan, B. Messer, M. Law, P.D. Yang, Adv. Mater. 14 (2002) 158.
[17] H. Ohta, M. Kamiya, T. Kamaiya, M. Hirano, H. Hosono, Thin Solid Films 445 (2003) 317.
[18] S.E. Ahn, J.S. Lee, H. Kim, S. Kim, B.H. Kang, K.H. Kim, G.T. Kim, Appl. Phys. Lett. 84 (2004) 5022.
[19] C.N.R. Rao, S.R.C. Vivekchand, K. Biswas, A. Govindaraj, Dalton Trans. (2007) 3728.
[20] C.N.R. Rao, A. Govindraj, Adv. Mater. 21 (2009) 4208.
[21] C.L. Wu, L. Chang, H.G. Chen, C.W. Lin, T.F. Chang, Y.C. Chao, J.K. Yan, Thin Solid Films 498 (2006) 137.
[22] X. Liu, X.H. Wu, H. Cao, R.P.H. Chang, J. Appl. Phys. 95 (2004) 3141.
[23] L.S. Panchakarla, A. Govindaraj, C.N.R. Rao, J. Cluster Sci. 18 (2007) 660.
[24] N. Varghese, L.S. Panchakarla, M. Hanapi, A. Govindaraj, C.N.R. Rao, Mater. Res. Bull. 42 (2007) 2117.
[25] L.S. Panchakarla, M.A. Shah, A. Govindraj, C.N.R. Rao, J. Solid State Chem. 180 (2007) 3106.
[26] J. Hu, R.G. Gordan, J. Appl. Phys. 71 (1992) 880.
[27] S.V. Prasad, S.D. Walck, J.S. Zabinski, Thin Solid Films 360 (2000) 107.
[28] T. Yoshida, H. Minoura, Adv. Mater. 12 (2000) 1219.
[29] A.B. Djurisic, Y.H. Leung, K.H. Tam, Y.F. Hsu, L. Ding, W.K. Ge, Y.C. Zhong, K.S. Wong, W.K. Chan, H.L. Tam, K.W. Cheah, W.M. Kwok, D.L. Phillips, Nanotechnology 18 (2007) 095702.
[30] X. Zhou, S. Gu, Z. Wu, S. Zhu, J. Ye, S. Liu, R. Zhang, Y. Shi, Y. Zheng, Appl. Surf. Sci. 253 (2006) 2226.
[31] H. Zeng, W. Cai, J. Hu, G. Duan, P. Liu, Y. Li, Appl. Phys. Lett. 88 (2006) 171910.
[32] K. Vanheusden, W.L. Warren, C.H. Seager, D.R. Tallant, J.A. Voigt, B.E. Gnade, J. Appl. Phys. 79 (1996) 7983.
[33] A. Sundaresan, R. Bhargavi, N. Rangarajan, U. Siddesh, C.N.R. Rao, Phys. Rev. B 74 (2006) 161306.
[34] A. Sundaresan, C.N.R. Rao, Nano Today 4 (2009) 96.
[35] A. Sundaresan, C.N.R. Rao, Solid State Commun. 149 (2009) 1197.